Available online at www.sciencedirect.com
SCIENCE DIRECT®
Journal of Solid State Chemistry 177 (2004) 1437–1443
JOURNAL OF SOLID STATE CHEMISTRY
http://elsevier.com/locate/jssc

The blue allotropic form of Co^{2+}:$Na_2CoP_2O_7$: optical and magnetic properties, correlation with crystallographic data

L. Beaury,[a,*] J. Derouet,[a] L. Binet,[a] F. Sanz,[b] and C. Ruiz-Valero[b]

[a] *Laboratoire de Chimie Appliquée de l'Etat Solide, CNRS-UMR 7574, ENSCP, 11 rue Pierre et Marie Curie, 75231 Paris Cedex 05, France*
[b] *ICMM-CSIC, Campus de Cantoblanco, Madrid 28049, Spain*

Received 23 September 2003; received in revised form 19 November 2003; accepted 23 November 2003

Abstract

$Na_2CoP_2O_7$ is found in two allotropic forms. The first one is rose and belongs to the triclinic crystallographic system. The second one is blue and described in the orthorhombic system, space group $Pna2_1$, No. 33, with cell parameters $a = 15.378(6)$ Å, $b = 10.271(4)$ Å, $c = 7.713(2)$ Å and $Z = 8$. A recent work showed that the orthorhombic phase could be considered as tetragonal: space group $P4_2/mnm$, No. 136 with $a = 7.706(1)$ Å and $b = 10.301(2)$ Å and $Z = 4$. The optical and magnetic properties, particularly the EPR spectrum, of the divalent cobalt ion and their phenomenological simulation were of considerable help to complement the study and allowed us to specify the real structure.

Keywords: Crystal field; Optical absorption; EPR; Sodium cobalt diphosphate; Magnetic susceptibility

1. Introduction

The mixed diphosphates containing both alkaline and divalent transition metal cations with the general formula $A_2MP_2O_7$ (A = Na, K and M = Co, Cu, Zn) and exhibiting the melilite structure type [1,2], have been indexed in the tetragonal system [3]. Among them the $Na_2CoP_2O_7$ compound has been particularly studied. Two new allotropic forms of this diphosphate have been characterized [4]: the first one is rose and belongs to the triclinic crystallographic system with a site symmetry C_1 for Co^{2+}, the second one is blue and orthorhombic with a site symmetry C_S for Co^{2+}. A recent work [5], performed by some of us, specified the characteristics of the so-called orthorhombic blue form. Indeed this compound seemed to be better described in the tetragonal system with a higher point symmetry (D_{2d}) for cobalt, which is unusual in inorganic solids [6]. The tetragonal form could then be a derivative of the orthorhombic form.

This paper reports on the analysis of optical and magnetic (susceptibility and electronic paramagnetic resonance (EPR)) properties of Co^{2+} ($3d^7$) in blue $Na_2CoP_2O_7$ in order to clarify the actual site symmetry for Co^{2+}. The powder optical absorption and EPR spectra, and the magnetic susceptibility are analyzed in terms of crystal field parameters using two approaches: (i) a semi-empirical calculation of the crystal field parameters (cfps) B_q^k from crystallographic data by the Simple Overlap Model (SOM) and (ii) simultaneous simulation of optical, paramagnetic and EPR data.

2. Crystallographic background

The $Na_2CoP_2O_7$ crystals were grown as described in Ref. [5]. This compound crystallizes in the tetragonal system, space group $P4_2/mnm$ (No. 136). It was found that the cell parameters are $a = 7.706(1)$ Å and $b = 10.301(2)$ Å and $Z = 4$. The Co^{2+} cation is located at the center of an axially distorted tetrahedron, whose point symmetry is D_{2d}. The distance between cobalt and oxygen O(2) is 1.956 Å. The CoO_4 tetrahedra are isolated and interconnected by bridging P_2O_7 groups through the O(2) oxygens and form a layered structure with Na cations between the layers (Fig. 1).

Erragh et al. [4] described $Na_2CoP_2O_7$ in the orthorhombic blue form (space group $Pna2_1$, No. 33). In this description, the cell parameters are $a = 15.378(6)$ Å,

*Corresponding author. Fax: +33-1-46-34-74-89.
E-mail address: beaury@ext.jussieu.fr (L. Beaury).

0022-4596/$ - see front matter © 2003 Elsevier Inc. All rights reserved.
doi:10.1016/j.jssc.2003.11.028

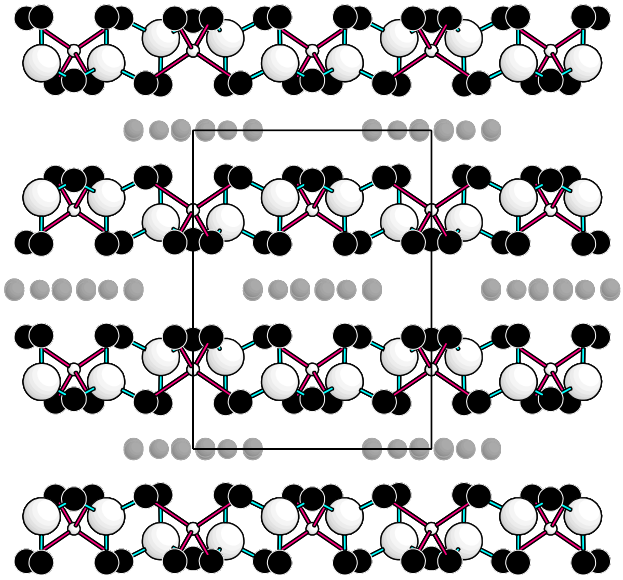

Fig. 1. View of the tetragonal $Na_2CoP_2O_7$ structure, showing the layered structure. The Na cations are represented by grey circles and oxygen atoms by dark filled circles. Small open circles represent cobalt atoms at the center of CoO_4 tetrahedra. Large open circles represent phosphorus atoms at the center of PO_4 tetrahedra (parts of P_2O_7 groups).

$b = 10.271(4)$ Å, $c = 7.713(2)$ Å and $Z = 8$. The Co^{2+} ions occupy two different sites Co1 and Co2 with same point symmetry C_1. The Co–O distances, in angstroms, are for Co1:

$$Co-O(3) = 1.9847,\ Co-O(12) = 1.9362,$$
$$Co-O(14) = 1.9671,\ Co-O(15) = 2.0018$$

and for Co2:

$$Co-O(2) = 1.9510,\ Co-O(6) = 1.8867,$$
$$Co-O(7) = 1.9513,\ Co-O(16) = 1.9552.$$

The structure is characterized by layers of mixed tetrahedra of CoO_4 and $P(PO_4)$ (thus $[CoP_2O_7]^{-2}$ layers) alternating with layers of sodium atoms.

3. Experimental background

The analysis by optical absorption was performed on polycrystalline powder of undoped $Na_2CoP_2O_7$ at 20 and 300 K with a Cary 2400 spectrophotometer in the 250–2500 nm wavelength range (Fig. 2).

The magnetic susceptibility was measured with a Quantum Design MPS-XL Squid magnetometer operating from 300 to 2 K at 5×10^{-5} T (Fig. 3) [5].

The compound $Na_2CoP_2O_7$ is not suitable for the EPR analysis since the strong magnetic interactions between close Co^{2+} would prevent the observation of the EPR signal of Co^{2+}. Therefore the isostructural compound $Na_2ZnP_2O_7$ doped with 1% of Co^{2+} was

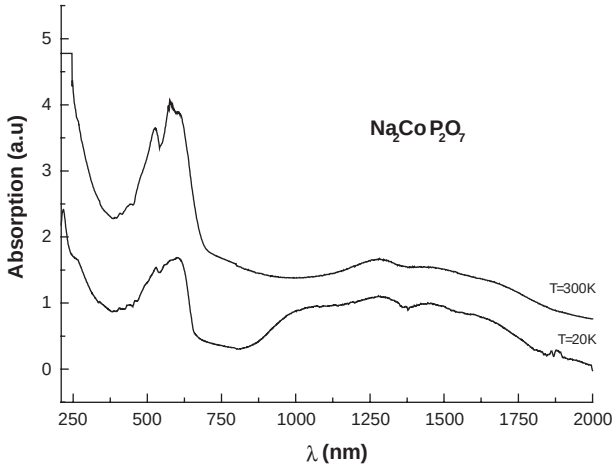

Fig. 2. Absorption spectra of $Na_2CoP_2O_7$ at 300 and 20 K.

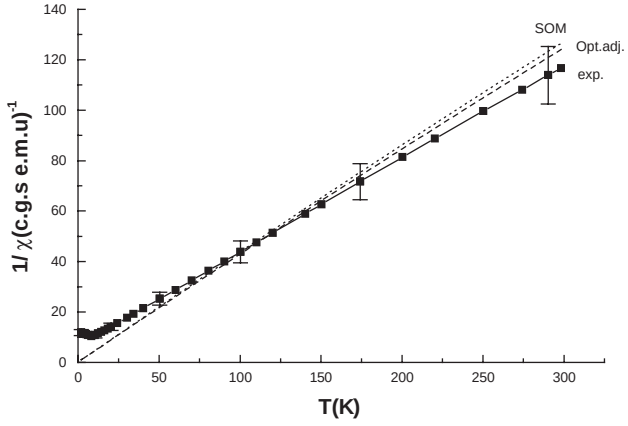

Fig. 3. Experimental (squares with errors bars of 10%) and computed reciprocal paramagnetic susceptibility versus temperature (dotted line: SOM calculation, dashed line: adjustment) for $Na_2CoP_2O_7$.

used in form of polycrystalline powder. The EPR spectra were recorded at various temperatures (between 4 and 300 K), in the 50–400 mT range, using a Bruker ESP 300e spectrometer equipped with a TE_{102} microwave cavity, and an ESR 9 helium flow cryostat from Oxford Instruments. A 100 kHz modulation of the magnetic field was used.

4. Theoretical background

4.1. The simple overlap model (semi-empirical calculations)

The Simple Overlap Model (SOM) developed by Malta [7–9], in which part of the chemical bonding is taken into account, has been applied successfully to reproduce the crystal field parameters (cfps) B_q^k for lanthanides as well as for 3*d* transition metal elements

[10–14]. In this model, the cfps are calculated from the atomic positions in the structure.

In this way, the crystal field effect can be calculated assuming a potential produced by an effective charge distribution q_j over a small region, proportional to the overlap ρ between the $3d$ orbitals of the central ion and the s and p orbitals of the ligands. The B_q^k parameters are calculated from the relation:

$$B_q^k = \rho\left(\frac{2}{1\pm\rho}\right)^{k+1} A_q^k \langle r^k \rangle$$

where A_q^k is the lattice sum of the neighbors belonging to the first coordination sphere and carrying an effective charge q_j, $\langle r^k \rangle$ are the radial integrals with $k \leqslant 2l$ (for cobalt, $\langle r^2 \rangle = 1.2587\,(\text{a.u.})^2$ and $\langle r^4 \rangle = 3.706\,(\text{a.u.})^4$ [15]).

The Simple Overlap Model is applied to the more difficult cases which make impossible the phenomenological simulation: (i) compounds with very low symmetry requiring the determination of 14 cfps, (ii) multisite character of the host matrix, (iii) puzzling questions on the d elements strongly affected by the phonons. Finally SOM may be regarded as a starting point to analyze optical properties as well as paramagnetic susceptibility or EPR spectra.

Once calculated from the crystal structure, the B_q^k are introduced into the diagonalization of the secular determinant of the $3d^7$ configuration, which involves 120 $|SLJM\rangle$ kets.

The description of the configuration is made on the $|SLJM\rangle$ basis although the $|SM_SLM_L\rangle$ basis is usually considered for the $3d$ elements with the introduction of the ligand field parameter $10Dq$ (instead of the individual B_q^k's). The latter is the separation between the two types of d orbitals d_γ and d_ε. The orbital d_γ (d_{z^2} and $d_{x^2}-d_{y^2}$) and d_ε (d_{xy}, d_{xz}, d_{yz}) are also denoted e and t_2 according to their associated irreducible representations in the T_d point group.

It is also useful to introduce the total ligand crystal field strength parameter S [16] which permits to compare the effect of different ligands:

$$S = \left[\frac{1}{n}\sum_k \sum_{q=-k}^{q=+k} \frac{1}{2k+1}(B_q^k)^2\right]^{1/2}$$

with $n = 2$ and $k = 2, 4$ for d elements.

4.2. Classical crystal-field calculation

The determinant of a $3d^N$ configuration is built on the $|SLJM\rangle$ basis. The Hamiltonian includes: (i) the free-ion interactions with the Coulombian repulsion H_{CR} characterized by Racah parameters B and C, the spin–orbit coupling H_{SO} characterized by the spin–orbit constant ζ [17], as well as the two- and three-body interactions and possibly the higher order spin–spin and spin-other-orbit interactions and (ii) the crystal field interaction H_{CF} which consists in a sum of products between the cfps and the spherical harmonics C_q^k:

$$H_{CF} = \sum_{k=0}^{4}\sum_{q=0}^{k} B_q^k[C_q^k + (-1)^q C_{-q}^k] + \mathrm{i}S_q^k[C_q^k - (-1)^q C_{-q}^k].$$

In the above expression, B_q^k and S_q^k represent the real and imaginary parts of the cfps. The number of non-zero parameters depends on the crystallographic site point symmetry. This method is almost completely described by Wybourne [18].

Generally the study of the $3d^N$ configurations frequently requires the use of the descending symmetry procedure, starting from the cubic symmetry which involves only the ligand field parameter Dq, directly related to B_0^4 by $B_0^4 = 21\,Dq$ for quaternary symmetry. The B_0^2 value and the deviation of the B_4^4/B_0^4 ratio from the cubic symmetry (in this case $|B_4^4/B_0^4| = 0.5976$) characterize the axial distortion.

As indicated before, the symmetries of the point sites are D_{2d} and C_1. Thus, we introduce the descending symmetry procedure $T_d \to D_{2d} \to C_{2v} \to C_s \to C_1$. The last two symmetry lowerings induce imaginary parts for the cfps (i.e. 14 cfps parameters which make impossible a phenomenological simulation). The diagonalization of the secular determinant leads to eigenvalues (energy levels) and to eigenfunctions. The latter are used to calculate the paramagnetic susceptibility and its variation versus temperature according to the van Vleck formula [19], and the magnetic g factors.

4.3. Magnetic splitting g factors

The $(\vec{L} + g_e\vec{S})$ tensorial operator is applied to the unperturbed wave function. The g values are non-zero only for Kramer's doublets. The general expression for g_z is written as:

$$g_z = 2[\langle \Psi_+|L_z + g_e S_z|\Psi_+\rangle^2 + \langle \Psi_+|L_z + g_e S_z|\Psi_-\rangle^2]^{1/2}.$$

For g_x and g_y, the expressions are similar. In the particular case of an axial symmetry there are only two different g values: $g_\parallel$ (parallel to the symmetry axis) $= g_z$ and $g_\perp = g_x = g_y$. In this expression Ψ_+ is a wave function of the form:

$$\Psi_+ = a|J, M\rangle + b|J, M'\rangle + \cdots,$$

whereas Ψ_- is its Kramer's conjugate.

5. Results and discussion

5.1. Optical absorption

Different bands, enlarged by a strong electron–phonon coupling, have been identified, and the charge transfer band edge starts at approximately 350 nm. It is however possible to deduce by decomposition an energy level scheme which is compatible with a $^4A_2$ ground state. The whole absorption spectrum shown in Fig. 2 is made of: (i) a very broad unresolved and weak band in the 2,000 nm (5,000 cm^{-1})–850 nm (11,800 cm^{-1}) range; this band could be a mixing between two spin-allowed transitions $^4A_2(^4F) \rightarrow {}^4T_2$, $^4T_1(^4F)$, and (ii) another broad band with a partly resolved structure in the 690–350 nm range (14,500–27,500 cm^{-1}). The latter is a mixing of allowed $^4A_2(^4F) \rightarrow {}^4T_1(^4P)$ and forbidden $^4A_2(^4F) \rightarrow {}^2E$, $^2T_1(^2G)$ transitions.

It is assumed that the tetrahedrally coordinated Co^{2+} ion ($3d^7$) can be described either in the D_{2d} or in the C_1 symmetries using the T_d notation. The d^7 configuration spans a serie of multiplets such as $^4F \Rightarrow {}^4A_2 + {}^4T_2 + {}^4T_1$ (orbitally non-degenerate ground state $^4A_2(^4F)$); $^4P \Rightarrow {}^4T_1$; $^2G \Rightarrow {}^2E + {}^2T_1 + {}^2A_1 + {}^2T_2$; $^2D \Rightarrow {}^2E + {}^2T_2$ and $^2H \Rightarrow {}^2E + {}^2T_1 + {}^2A_1 + {}^2T_2$. From the Tanabe-Sugano diagrams, we can expect to observe the transitions from the $^4A_2(^4F)$ ground state to the excited states mentioned above. We can notice that the transition $^4A_2(^4F) \rightarrow {}^4T_2(^4F)$, forbidden in T_d symmetry, can be observed for a distorted site with a very weak intensity. For all the transitions, a coupling with vibrational modes of the entity $[P_2O_7]^{4-}$ ($v = 832\,cm^{-1}$) can be expected. From the estimated positions of the allowed transitions, we can evaluate the usual spectroscopic parameters: the Dq crystal field parameter and the free-ion Racah parameter B related only to electronic transitions. However, despite the common use, these values are not correct because they are determined from the maximum of the absorption bands, but they do not take into account the position of the vibronically coupled levels due to Stokes shifts.

In order to determine the specific values of Dq and B from allowed experimental transitions one uses the expression of the energy levels given by König [20]. In the case of d^7 tetrahedral site (octahedral d^3), these expressions are written as follows:

$$v_1 = 10Dq, \tag{1}$$

$$v_2 = \tfrac{1}{2}(15B + 30Dq) - \tfrac{1}{2}[(15B - 10Dq)^2 + 12B.10Dq]^{1/2}, \tag{2}$$

$$v_3 = \tfrac{1}{2}(15B + 30Dq) + \tfrac{1}{2}[(15B - 10Dq)^2 + 12B.10Dq]^{1/2}. \tag{3}$$

In our case, we can notice that the $^4A_2 \rightarrow {}^4T_2(^4F)$ transition at v_1 cannot be clearly identified in the absorption spectrum. This transition could be situated near the $^4A_2 \rightarrow {}^4T_1(^4F)$ transition at v_2. The great difficulty is linked to the presence of the cobalt in several sites and to the broadening and shift due to the dual electronic/vibrational character. Therefore it is more convenient to calculate B and Dq from the positions of the v_2 $[^4A_2 \rightarrow {}^4T_1(^4F)]$ transition in the $8,500 - 11,000\,cm^{-1}$ range and of the v_3 $[^4A_2(^4F) \rightarrow {}^4T_1(^4P)]$ transition, strongly mixed with the $^4A_2(^4F) \rightarrow {}^4E, {}^2T_1(^2G)$ forbidden transition in the $14,700 - 20,000\,cm^{-1}$ range. As an example the energy level ^4P at 18,987 cm^{-1} is a mixture of 66% (^4P) and 34% (^2G). Consequently the parameters B and $10Dq$ can be calculated from:

$$B = \frac{1}{510}[7(v_2 + v_3) \pm \{49(v_2 + v_3)^2 + 680(v_2 - v_3)^2\}^{1/2}],$$

$$10Dq = \tfrac{1}{3}(v_2 + v_3) - 5B.$$

With this hypothesis, the most likely values are $B = 739\,cm^{-1}$ in agreement with the value 700 cm^{-1} in a pseudo-tetrahedral site [14] and $Dq \cong 501\,cm^{-1}$.

Despite the very bad absorption spectrum, it is possible to deduce a rough energy level scheme: (i) by decomposition of the two broad bands v_2 and v_3 as mentioned above and (ii) from the position of the weak forbidden transitions observed in the 20,000–31,000 cm^{-1} range.

In a first step to confirm our representation, we performed an analysis of the absorption spectrum on the basis of the crystal model (phenomenological simulation). The number 21 of observed levels is not sufficient to consider the exact C_S point symmetry of Co^{2+}. The calculation is then carried out with the D_{2d} symmetry (tetragonal phase). The involved parameters consist of three free ion parameters B, C and ζ, and three real crystal field parameters B_0^2, B_0^4 and B_4^4. The results are reported in Table 1.

With this set of calculated parameters, we obtained the magnetic susceptibility (Fig. 3) and the $g_{\parallel}$ and $g_{\perp}$ values (Table 2).

5.2. Crystallographic data (SOM calculation)

In order to calculate the cfps in the distorted tetragonal symmetry of cobalt in $Na_2CoP_2O_7$, a systematic assessment of the multi-dimensional space involving the B_q^k, the oxygen effective charge q_j and the overlap ρ was done for the two point symmetries D_{2d} (one site) and C_S (two sites). The calculations of the effective charge q_j attributed to each oxygen of the first coordination sphere (Table 3) are performed using the

Table 1
Parameters (cm^{-1}) for $Na_2CoP_2O_7$

Parameter	Exp	Optical adjust D_{2d}	SOM calculation		
			Tetra D_{2d}	Orthorhombic C_1	
				Co1	Co2
ρ			0.13	0.13	0.13
q_j			−0.8	−0.8	−0.9
B_0^2		−1655	−1896	−2847	−1304
B_1^2				−693	821
B_1^2 Im				1509	3
B_2^2				−211	459
B_2^2 Im				−1201	808
B_0^4	−10521	−9558	−10412	−10853	−10592
B_1^4				183	−3931
B_1^4 Im				−1494	125
B_2^4				−1931	1914
B_2^4 Im				−1113	494
B_3^4				−769	1150
B_3^4 Im				899	421
B_4^4		7901	8022	8724	8203
B_4^4 Im				2086	−998
B_4^4/B_0^4		−0.83	−0.77	−0.80	−0.77
Total strength S			3809	4255	4077
Rms		147			
Nb levels		21			
B	739	716	716	716	716
C[a]		3479	3479	3479	3479
C/B		4.86	4.86	4.86	4.86
Dq	501	455	496	517	504
Dq/B	0.68	0.64	0.69	0.72	0.70

Note. The spin–orbit coupling constant ζ is set at 410 cm^{-1} (80% of the free ion value) [21].

[a] The Racah parameter C varies around the hydrogenic ratio $C \cong 4B$ [20] and can be determined from the spin-forbidden transitions.

Table 2
Experimental and calculated g values

Experimental values	Optical adjust. (D_{2d})	SOM calculation		
		Tetrahedral sym.	Orthorhombic sym.	
			Co1	Co2
6.4				
5.8				$g_x = 5.73$
5.3			$g_x = 5.38$	
4.9				
4.6	$g_\perp = 4.44$	$g_\perp = 4.41$		
3.1			$g_y = 3.07$	
				$g_y = 2.57$
2.3–2.0	$g_\parallel = 2.17$	$g_\parallel = 2.17$	$g_z = 2.33$	$g_z = 2.02$

formula [22]:

$$q_j = \exp\left(\frac{r_0 - r_j}{\beta}\right) \text{(e.s.u.)},$$

where r_j is the metal–ligand distance, r_0 is the mean radius of a given ligand-type coordination sphere surrounding a given cation. According to Brown [22], r_0 is about 1.692 Å for Co–O bond and β is a parameter whose value varies slightly around 0.37 whatever the material. In this study, the best results are obtained with $r_0 = 1.895$ Å and $\beta = 0.37$, and for an oxygen mean effective charge $-0.9 < q_{jm} < -0.8$. These values are very close to effective charges found for the oxygen ligands of lanthanides compounds [13] and for other phosphates of divalent cobalt [12]. For the 3d elements, the overlap is usually assumed to be in the range 0.10–0.20 which is much higher than in the case of the rare-earth ions ($0.05 \leqslant \rho \leqslant 0.08$).

Table 3
Bond distances (Å) and effective charges for $Na_2CoP_2O_7$

	d (Co–O)	Effective charge q_j	Mean effective charge q_{jm}
Tetra	Co–O = 1.9562	−0.848	−0.848
Ortho Co1	Co–O(3) = 1.9847	−0.785	
	Co–O(12) = 1.9362	−0.895	
	Co–O(14) = 1.9671	−0.760	−0.797
	Co–O(15) = 2.0018	−0.749	
Ortho Co2	Co–O(2) = 1.9510	−0.86	
	Co–O(6) = 1.8867	−1.023	
	Co–O(7) = 1.9513	−0.859	−0.898
	Co–O(16) = 1.9552	−0.850	

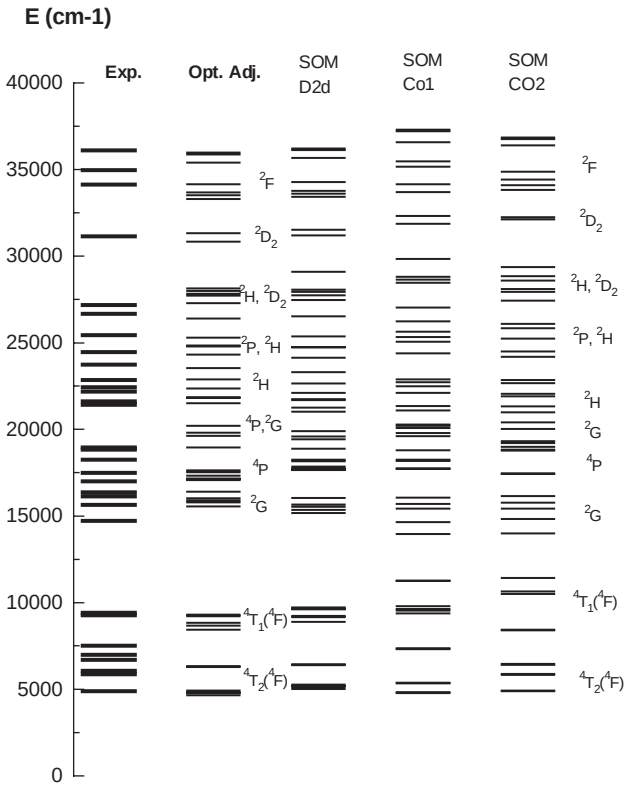

Fig. 4. Experimental and calculated energy level scheme.

The range $0.12 \leqslant \rho \leqslant 0.15$ turns to be the best choice to reproduce correctly optical and magnetic properties with the parameters reported in Table 1. The complete energy level scheme of Co^{2+} (zero-phonon lines) calculated with $\rho = 0.13$ (Fig. 4) is in good agreement with the experimental one in spite of the mediocrity of the latter. Contrary to the case of lanthanides, we underline the impossibility to characterize an energy level only with a single $|SLJM\rangle$ ket. An important mixing is noted between the nominal states $^2E(^2G), ^2T_1(^2G), ^4T_1(^4P)$. As an example the wavefunction associated to one component with the label "^4P" at 18,987 cm^{-1} for Co2 in orthorhombic symmetry can be expanded as:

$$0.66|^4P, ^4F\rangle + 0.34|^2P, ^2D, ^2G, ^2H\rangle.$$

5.3. Paramagnetic susceptibility

The paramagnetic susceptibility χ is calculated according to the van Vleck formula [17,23]. The used wavefunctions are derived from the sets of parameters obtained above (Table 1). The calculated and experimental average values are plotted in Fig 3, which shows the temperature dependence of the reciprocal magnetic susceptibility of the $Na_2CoP_2O_7$ sample.

The three sites occupied by Co^{2+} almost lead to the same curve, which is very slightly different from the one obtained by optical adjustment. The agreement between calculated and experimental values is fairly good in the 25–300 K range, corresponding to a Curie–Weiss law. The calculated magnetic moment takes the values 4.24–4.34 BM, respectively.

We can remark that χ reaches a constant value at low temperature. The deviation from the Curie–Weiss behavior below about 10 K could be due to the onset of antiferromagnetic interactions in the Co^{2+} sublattice of this material [5]. This "spoon shape" was previously observed in Neodymium [24]. The calculation shows that $1/\chi_{x,y}$ or $1/\chi_{\perp} \to 0$, though $1/\chi_z$ or $1/\chi_{\|} \to C^{te}$.

The calculated ZFS (zero field splitting) values are 5 cm^{-1} for the tetragonal site, and 4 and 9 cm^{-1} for the two orthorhombic sites Co1 and Co2 respectively.

5.4. EPR investigations

Fig. 5 shows the evolution between 4 and 300 K of the EPR spectrum of the compound $Na_2ZnP_2O_7$:Co^{2+}. The signal is dramatically temperature dependent. At low temperature, we first observe a strong line at about 140 mT corresponding to $g = 4.6$ along with a weaker component at about 300 mT corresponding to $g = 2.3$. Both components are typical of a paramagnetic species in axial symmetry with effective spin $S = 1/2$ and thus can be attributed to cobalt in tetrahedral site. The other EPR lines could corroborate the presence of the two orthorhombic sites previously described. At room temperature, the tetrahedral signal almost vanishes and the shape of the spectrum in the highest field range ($\sim$340 mT) seems to be due to an additional species exhibiting resolved hyperfine interaction.

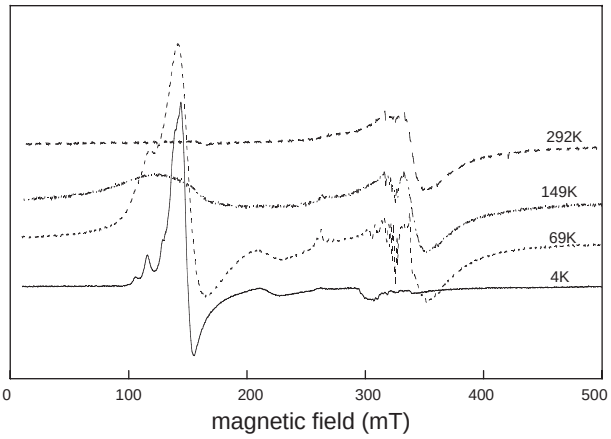

Fig. 5. Experimental EPR spectra at 292, 149, 69, 4 K for $Na_2ZnP_2O_7$: Co^{2+}.

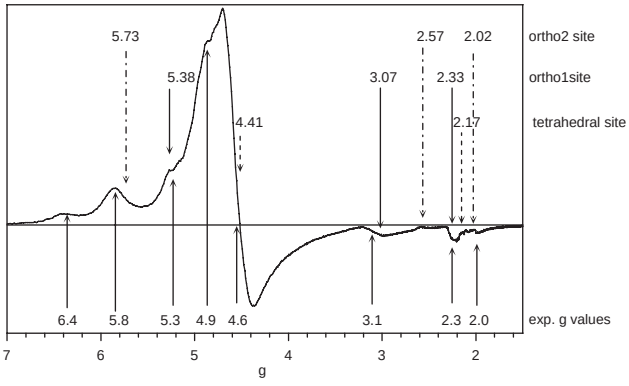

Fig. 6. Experimental EPR spectrum at 4 K with experimental and calculated g values.

The experimental g values determined from the EPR spectrum at 4 K (Fig. 6) are reported in Table 2. The uncertainty on these values is about 0.1.

The g values calculated with the parameters of Table 1 from optical adjustment and SOM calculation are also given in Table 2.

The EPR spectrum at 4 K (Figs. 5 and 6) indicates the existence of more cobalt species than expected from the crystal structure. More specifically, the EPR features at $g = 6.4$ and 4.9 do not correspond to any calculated value and could possibly arise from a parasitic phase undetected by X-ray diffraction.

The agreement between the calculated value of $g_{\perp}$ for Co^{2+} in tetrahedral site or the calculated values of g_x for Co^{2+} in orthorhombic sites and the corresponding experimental values can be considered as satisfactory, given the uncertainties on the experimental g values. The

calculated value $g_y = 3.07$ for Co1 matches also fairly well the experimental value $g = 3.1$. However the calculated value $g_y = 2.57$ for Co2 does not correspond to any experimental value. Indeed the small bump at $g = 2.57$ on the spectrum in Fig. 6 rather corresponds to the additional species predominating at higher temperatures (Fig. 5) and not to Co2. The actual value of g_y for Co2 is probably close to 3.0–3.1 and the corresponding EPR component could then be superimposed with that of Co1. The agreement between the calculated values of $g_{\|}$ in tetrahedral site or the values of g_z for Co1 and Co2 and the experimental values is more difficult to assess due to the weakness of the EPR signal in this g value range and the overlap with the signal of the species seen at higher temperature. Notwithstanding, there seems to be a slight discrepancy between the value $g_{\|} = 2.17$ calculated for Co^{2+} in tetrahedral site which rather seems to be about 2.3 from the experimental spectrum.

The strong covalence of cobalt could account for some discrepancies between experimental and calculated g values (SOM calculation).

6. Conclusion

Optical spectrum and magnetic susceptibility are weakly dependent on the wavefunction but the g factors are very sensitive to the composition of the ground state wavefunction, i.e. to the values of crystal field parameters. The experimental EPR spectrum reveals that the Co^{2+} cannot be considered only in a tetragonal symmetry. This very complex spectrum can be explained considering for Co^{2+} a predominant tetrahedral site, two orthorhombic sites and probably others parasitic phases.

References

[1] M. Kimata, Neues JahrB. Miner. 146 (1983) 221–224.
[2] K. Hagiya, M. Ohmasa, K. Iishi, Acta Crystallogr. B 49 (1993) 172–179.
[3] M. Gabelica-Robert, C. R. Acad. Sci. Paris 293 (1981) 497–499.
[4] F. Erragha, A. Boukhari, B. El Ouadi, E.M. Holt, J. Crystallogr. Spectrosc. Res. 21 (1991) 321–326.
[5] F. Sanz, C. Ruiz Valero, J.M. Rojo, C. Parada, R. Saez-Puche, J. Solid State Chem. 145 (1999) 604–611.
[6] M. Wildner, Z. Kristallogr. 205 (1992) 51–70.
[7] O.L. Malta, Chem. Phys. Lett. 87 (1982) 27–29.
[8] O.L. Malta, Chem. Phys. Lett. 88 (1983) 353–356.
[9] R.Q. Albuquerque, G.B. Rocha, O.L. Malta, P. Porcher, Chem. Phys. Lett. 331 (2000) 519–525.
[10] O.L. Malta, G.F. De Sa, Quim. Nova (Brazil) 6 (1983) 123–124.
[11] O.L. Malta, S.L.J. Ribeiro, M. Faucher, P. Porcher, J. Phys. Chem. Solids 52 (1991) 587–593.
[12] J. Derouet, L. Beaury, P. Porcher, R. Olazcuaga, J.M. Dance, G. Leflem, M. El Bouari, A. El Jazouli, J. Solid State Chem. 143 (1999) 230–238.
[13] P. Porcher, M.A. Couto dos Santos, O. Malta, Phys. Chem. Chem. Phys. 1 (1999) 397–405.
[14] J. Derouet, L. Beaury, P. Porcher, P.J. Deren, J. Alloys. Compd. 300–301 (2000) 242–253.
[15] S. Fraga, J. Karkowski, K.M.S. Saxena, Handbook of Atomic Data, Elsevier, Amsterdam, 1976.
[16] F. Auzel, O. Malta, J. Phys. 44 (1983) 201–206.
[17] B.N. Figgis, Introduction to Ligand Fields, Interscience, New York, 1966.
[18] B.G. Wybourne, Spectroscopic Properties of Rare Earths Ions, Interscience, New York, 1965.
[19] J.H. van Vleck, J. Appl. Phys. 39 (1968) 365–374.
[20] E. König, Struct. Bond. (Berlin) 9 (1971) 175–212.
[21] E. König, S. Kremer, Ber. Bunsenges. 78 (8) (1974) 786–795.
[22] D. Brown, D. Altermatt, Acta Crystallogr. B 41 (1985) 244–247, internet data.
[23] L. Beaury, J. Derouet, M. Escorne, P. Porcher, J. Phys.: Condens. Matter 6 (1994) 5169–5180.
[24] J. Derouet, L. Beaury, P. Porcher, J. Alloys. Compd. 323–324 (2001) 460–467.